# $J/\psi$ Production from Proton-Proton Collisions at $\sqrt{s} = 200$ GeV

S. S. Adler,[5] S. Afanasiev,[17] C. Aidala,[5] N. N. Ajitanand,[43] Y. Akiba,[20,38] J. Alexander,[43] R. Amirikas,[12] L. Aphecetche,[45] S. H. Aronson,[5] R. Averbeck,[44] T. C. Awes,[35] R. Azmoun,[44] V. Babintsev,[15] A. Baldisseri,[10] K. N. Barish,[6] P. D. Barnes,[27] B. Bassalleck,[33] S. Bathe,[30] S. Batsouli,[9] V. Baublis,[37] A. Bazilevsky,[39,15] S. Belikov,[16,15] Y. Berdnikov,[40] S. Bhagavatula,[16] J. G. Boissevain,[27] H. Borel,[10] S. Borenstein,[25] M. L. Brooks,[27] D. S. Brown,[34] N. Bruner,[33] D. Bucher,[30] H. Buesching,[30] V. Bumazhnov,[15] G. Bunce,[5,39] J. M. Burward-Hoy,[26,44] S. Butsyk,[44] X. Camard,[45] J.-S. Chai,[18] P. Chand,[4] W. C. Chang,[2] S. Chernichenko,[15] C. Y. Chi,[9] J. Chiba,[20] M. Chiu,[9] I. J. Choi,[52] J. Choi,[19] R. K. Choudhury,[4] T. Chujo,[5] V. Cianciolo,[35] Y. Cobigo,[10] B. A. Cole,[9] P. Constantin,[16] D. G. d'Enterria,[45] G. David,[5] H. Delagrange,[45] A. Denisov,[15] A. Deshpande,[39] E. J. Desmond,[5] O. Dietzsch,[41] O. Drapier,[25] A. Drees,[44] K. A. Drees,[5] R. du Rietz,[29] A. Durum,[15] D. Dutta,[4] Y. V. Efremenko,[35] K. El Chenawi,[49] A. Enokizono,[14] H. En'yo,[38,39] S. Esumi,[48] L. Ewell,[5] D. E. Fields,[33,39] F. Fleuret,[25] S. L. Fokin,[23] B. D. Fox,[39] Z. Fraenkel,[51] J. E. Frantz,[9] A. Franz,[5] A. D. Frawley,[12] S.-Y. Fung,[6] S. Garpman,[29,*] T. K. Ghosh,[49] A. Glenn,[46] G. Gogiberidze,[46] M. Gonin,[25] J. Gosset,[10] Y. Goto,[39] R. Granier de Cassagnac,[25] N. Grau,[16] S. V. Greene,[49] M. Grosse Perdekamp,[39] W. Guryn,[5] H.-Å. Gustafsson,[29] T. Hachiya,[14] J. S. Haggerty,[5] H. Hamagaki,[8] A. G. Hansen,[27] E. P. Hartouni,[26] M. Harvey,[5] R. Hayano,[8] X. He,[13] M. Heffner,[26] T. K. Hemmick,[44] J. M. Heuser,[44] M. Hibino,[50] J. C. Hill,[16] W. Holzmann,[43] K. Homma,[14] B. Hong,[22] A. Hoover,[34] T. Ichihara,[38,39] V. V. Ikonnikov,[23] K. Imai,[24,38] D. Isenhower,[1] M. Ishihara,[38] M. Issah,[43] A. Isupov,[17] B. V. Jacak,[44] W. Y. Jang,[22] Y. Jeong,[19] J. Jia,[44] O. Jinnouchi,[38] B. M. Johnson,[5] S. C. Johnson,[26] K. S. Joo,[31] D. Jouan,[36] S. Kametani,[8,50] N. Kamihara,[47,38] J. H. Kang,[52] S. S. Kapoor,[4] K. Katou,[50] S. Kelly,[9] B. Khachaturov,[51] A. Khanzadeev,[37] J. Kikuchi,[50] D. H. Kim,[31] D. J. Kim,[52] D. W. Kim,[19] E. Kim,[42] G.-B. Kim,[25] H. J. Kim,[52] E. Kistenev,[5] A. Kiyomichi,[48] K. Kiyoyama,[32] C. Klein-Boesing,[30] H. Kobayashi,[38,39] L. Kochenda,[37] V. Kochetkov,[15] D. Koehler,[33] T. Kohama,[14] M. Kopytine,[44] D. Kotchetkov,[6] A. Kozlov,[51] P. J. Kroon,[5] C. H. Kuberg,[1,27] K. Kurita,[39] Y. Kuroki,[48] M. J. Kweon,[22] Y. Kwon,[52] G. S. Kyle,[34] R. Lacey,[43] V. Ladygin,[17] J. G. Lajoie,[16] A. Lebedev,[16,23] S. Leckey,[44] D. M. Lee,[27] S. Lee,[19] M. J. Leitch,[27] X. H. Li,[6] H. Lim,[42] A. Litvinenko,[17] M. X. Liu,[27] Y. Liu,[36] C. F. Maguire,[49] Y. I. Makdisi,[5] A. Malakhov,[17] V. I. Manko,[23] Y. Mao,[7,38] G. Martinez,[45] M. D. Marx,[44] H. Masui,[48] F. Matathias,[44] T. Matsumoto,[8,50] P. L. McGaughey,[27] E. Melnikov,[15] F. Messer,[44] Y. Miake,[48] J. Milan,[43] T. E. Miller,[49] A. Milov,[44,51] S. Mioduszewski,[5] R. E. Mischke,[27] G. C. Mishra,[13] J. T. Mitchell,[5] A. K. Mohanty,[4] D. P. Morrison,[5] J. M. Moss,[27] F. Mühlbacher,[44] D. Mukhopadhyay,[51] M. Muniruzzaman,[6] J. Murata,[38,39] S. Nagamiya,[20] J. L. Nagle,[9] T. Nakamura,[14] B. K. Nandi,[6] M. Nara,[48] J. Newby,[46] P. Nilsson,[29] A. S. Nyanin,[23] J. Nystrand,[29] E. O'Brien,[5] C. A. Ogilvie,[16] H. Ohnishi,[5,38] I. D. Ojha,[49,3] K. Okada,[38] M. Ono,[48] V. Onuchin,[15] A. Oskarsson,[29] I. Otterlund,[29] K. Oyama,[8] K. Ozawa,[8] D. Pal,[51] A. P. T. Palounek,[27] V. S. Pantuev,[44] V. Papavassiliou,[34] J. Park,[42] A. Parmar,[33] S. F. Pate,[34] T. Peitzmann,[30] J.-C. Peng,[27] V. Peresedov,[17] C. Pinkenburg,[5] R. P. Pisani,[5] F. Plasil,[35] M. L. Purschke,[5] A. K. Purwar,[44] J. Rak,[16] I. Ravinovich,[51] K. F. Read,[35,46] M. Reuter,[44] K. Reygers,[30] V. Riabov,[37,40] Y. Riabov,[37] G. Roche,[28] A. Romana,[25] M. Rosati,[16] P. Rosnet,[28] S. S. Ryu,[52] M. E. Sadler,[1] N. Saito,[38,39] T. Sakaguchi,[8,50] M. Sakai,[32] S. Sakai,[48] V. Samsonov,[37] L. Sanfratello,[33] R. Santo,[30] H. D. Sato,[24,38] S. Sato,[5,48] S. Sawada,[20] Y. Schutz,[45] V. Semenov,[15] R. Seto,[6] M. R. Shaw,[1,27] T. K. Shea,[5] T.-A. Shibata,[47,38] K. Shigaki,[14,20] T. Shiina,[27] C. L. Silva,[41] D. Silvermyr,[27,29] K. S. Sim,[22] C. P. Singh,[3] V. Singh,[3] M. Sivertz,[5] A. Soldatov,[15] R. A. Soltz,[26] W. E. Sondheim,[27] S. P. Sorensen,[46] I. V. Sourikova,[5] F. Staley,[10] P. W. Stankus,[35] E. Stenlund,[29] M. Stepanov,[34] A. Ster,[21] S. P. Stoll,[5] T. Sugitate,[14] J. P. Sullivan,[27] E. M. Takagui,[41] A. Taketani,[38,39] M. Tamai,[50] K. H. Tanaka,[20] Y. Tanaka,[32] K. Tanida,[38] M. J. Tannenbaum,[5] P. Tarján,[11] J. D. Tepe,[1,27] T. L. Thomas,[33] J. Tojo,[24,38] H. Torii,[24,38] R. S. Towell,[1] I. Tserruya,[51] H. Tsuruoka,[48] S. K. Tuli,[3] H. Tydesjö,[29] N. Tyurin,[15] H. W. van Hecke,[27] J. Velkovska,[5,44] M. Velkovsky,[44] L. Villatte,[46] A. A. Vinogradov,[23] M. A. Volkov,[23] E. Vznuzdaev,[37] X. R. Wang,[13] Y. Watanabe,[38,39] S. N. White,[5] F. K. Wohn,[16] C. L. Woody,[5] W. Xie,[6] Y. Yang,[7] A. Yanovich,[15] S. Yokkaichi,[38,39] G. R. Young,[35] I. E. Yushmanov,[23] W. A. Zajc,[9,†] C. Zhang,[9] S. Zhou,[7] S. J. Zhou,[51] and L. Zolin[17]

(PHENIX Collaboration)

[1]*Abilene Christian University, Abilene, Texas 79699, USA*
[2]*Institute of Physics, Academia Sinica, Taipei 11529, Taiwan*
[3]*Department of Physics, Banaras Hindu University, Varanasi 221005, India*
[4]*Bhabha Atomic Research Centre, Bombay 400 085, India*

 0031-9007/04/92(5)/051802(6)$22.50  

[5]*Brookhaven National Laboratory, Upton, New York 11973-5000, USA*
[6]*University of California–Riverside, Riverside, California 92521, USA*
[7]*China Institute of Atomic Energy (CIAE), Beijing, People's Republic of China*
[8]*Center for Nuclear Study, Graduate School of Science, University of Tokyo, 7-3-1 Hongo, Bunkyo, Tokyo 113-0033, Japan*
[9]*Columbia University, New York, New York 10027, USA, and Nevis Laboratories, Irvington, New York 10533, USA*
[10]*Dapnia, CEA Saclay, F-91191, Gif-sur-Yvette, France*
[11]*Debrecen University, H-4010 Debrecen, Egyetem tér 1, Hungary*
[12]*Florida State University, Tallahassee, Florida 32306, USA*
[13]*Georgia State University, Atlanta, Georgia 30303, USA*
[14]*Hiroshima University, Kagamiyama, Higashi-Hiroshima 739-8526, Japan*
[15]*Institute for High Energy Physics (IHEP), Protvino, Russia*
[16]*Iowa State University, Ames, Iowa 50011, USA*
[17]*Joint Institute for Nuclear Research, 141980 Dubna, Moscow Region, Russia*
[18]*KAERI, Cyclotron Application Laboratory, Seoul, South Korea*
[19]*Kangnung National University, Kangnung 210-702, South Korea*
[20]*KEK, High Energy Accelerator Research Organization, Tsukuba-shi, Ibaraki-ken 305-0801, Japan*
[21]*KFKI Research Institute for Particle and Nuclear Physics (RMKI), H-1525 Budapest 114, POBox 49, Hungary*
[22]*Korea University, Seoul, 136-701, Korea*
[23]*Russian Research Center "Kurchatov Institute," Moscow, Russia*
[24]*Kyoto University, Kyoto 606, Japan*
[25]*Laboratoire Leprince-Ringuet, Ecole Polytechnique, CNRS-IN2P3, Route de Saclay, F-91128, Palaiseau, France*
[26]*Lawrence Livermore National Laboratory, Livermore, California 94550, USA*
[27]*Los Alamos National Laboratory, Los Alamos, New Mexico 87545, USA*
[28]*LPC, Université Blaise Pascal, CNRS-IN2P3, Clermont-Fd, 63177 Aubiere Cedex, France*
[29]*Department of Physics, Lund University, Box 118, SE-221 00 Lund, Sweden*
[30]*Institut fuer Kernphysik, University of Muenster, D-48149 Muenster, Germany*
[31]*Myongji University, Yongin, Kyonggido 449-728, Korea*
[32]*Nagasaki Institute of Applied Science, Nagasaki-shi, Nagasaki 851-0193, Japan*
[33]*University of New Mexico, Albuquerque, New Mexico 87131, USA*
[34]*New Mexico State University, Las Cruces, New Mexico 88003, USA*
[35]*Oak Ridge National Laboratory, Oak Ridge, Tennessee 37831, USA*
[36]*IPN-Orsay, Universite Paris Sud, CNRS-IN2P3, BP1, F-91406, Orsay, France*
[37]*PNPI, Petersburg Nuclear Physics Institute, Gatchina, Russia*
[38]*RIKEN (The Institute of Physical and Chemical Research), Wako, Saitama 351-0198, Japan*
[39]*RIKEN BNL Research Center, Brookhaven National Laboratory, Upton, New York 11973-5000, USA*
[40]*St. Petersburg State Technical University, St. Petersburg, Russia*
[41]*Universidade de São Paulo, Instituto de Física, Caixa Postal 66318, São Paulo CEP05315-970, Brazil*
[42]*System Electronics Laboratory, Seoul National University, Seoul, South Korea*
[43]*Chemistry Department, Stony Brook University, SUNY, Stony Brook, New York 11794-3400, USA*
[44]*Department of Physics and Astronomy, Stony Brook University, SUNY, Stony Brook, New York 11794, USA*
[45]*SUBATECH (Ecole des Mines de Nantes, CNRS-IN2P3, Université de Nantes), BP 20722-44307, Nantes, France*
[46]*University of Tennessee, Knoxville, Tennessee 37996, USA*
[47]*Department of Physics, Tokyo Institute of Technology, Tokyo, 152-8551, Japan*
[48]*Institute of Physics, University of Tsukuba, Tsukuba, Ibaraki 305, Japan*
[49]*Vanderbilt University, Nashville, Tennessee 37235, USA*
[50]*Waseda University, Advanced Research Institute for Science and Engineering, 17 Kikui-cho, Shinjuku-ku, Tokyo 162-0044, Japan*
[51]*Weizmann Institute, Rehovot 76100, Israel*
[52]*Yonsei University, IPAP, Seoul 120-749, Korea*
(Received 8 July 2003; published 5 February 2004)

$J/\psi$ production has been measured in proton-proton collisions at $\sqrt{s} = 200$ GeV over a wide rapidity and transverse momentum range by the PHENIX experiment at the Relativistic Heavy Ion Collider. Distributions of the rapidity and transverse momentum, along with measurements of the mean transverse momentum and total production cross section are presented and compared to available theoretical calculations. The total $J/\psi$ cross section is $4.0 \pm 0.6(\text{stat}) \pm 0.6(\text{syst}) \pm 0.4(\text{abs})$ $\mu$b. The mean transverse momentum is $1.80 \pm 0.23(\text{stat}) \pm 0.16(\text{syst})$ GeV/$c$.

DOI: 10.1103/PhysRevLett.92.051802 PACS numbers: 13.85.Ni, 13.20.Fc, 14.40.Gx, 25.75.Dw

Understanding $J/\psi$ production mechanisms requires data over a large range of collision energies and with broad coverage in rapidity and transverse momentum ($p_T$). Existing data at lower energies from fixed target hadron experiments yield total cross sections and mean $p_T$ ($\langle p_T \rangle$) values in the energy range $\sqrt{s} = 7$–$38.8$ GeV [1]. Limited kinematic coverage in collider experiments [1–3] has so far meant that total cross sections and mean

$p_T$ values could not be measured. The systematic study of $J/\psi$ production at Relativistic Heavy Ion Collider (RHIC) energies with wide $p_T$ and rapidity coverage should therefore provide crucial tests of $J/\psi$ production models. In addition, the RHIC proton-proton results provide a baseline for studying cold and hot nuclear matter in proton-nucleus and nucleus-nucleus collisions using $J/\psi$ yields as a probe.

Intense theoretical interest in the $J/\psi$ production mechanism was stimulated when the color singlet model (CSM) was found [4] to dramatically underpredict the high $p_T$ prompt $J/\psi$ and $\psi(2S)$ cross sections measured with the collider detector at Fermilab (CDF) [3]. Attention turned toward models in which color octet $c\bar{c}$ states can also contribute to the $J/\psi$ yield. The color octet model (COM), which is based on the nonrelativistic QCD (NRQCD) approach [5], has been successful in reproducing the high $p_T$ CDF prompt $J/\psi$ cross sections, as has the more phenomenological color evaporation model (CEM) [6].

In this Letter we report results of the first measurements of $pp \to J/\psi + X$ at RHIC, made at $\sqrt{s} = 200$ GeV by the PHENIX experiment. The data yield the first total cross sections for $J/\psi$ production beyond fixed target energies, and the first measurement of $\langle p_T \rangle$ beyond $\sqrt{s} =$ 63 GeV. They will constrain models in the lower $p_T$ region where gluon fusion is expected to dominate. At $p_T$ beyond about 5 GeV/c, the direct $J/\psi$ production cross section is expected to be dominated by fragmentation of high $p_T$ gluons [7].

The PHENIX experiment [8] detects electrons in the pseudorapidity range $|\eta| \leq 0.35$ in two central spectrometer arms covering $\Delta\phi = 90°$, and forward rapidity muons in two muon arms covering $\Delta\phi = 360°$. Only one muon arm, covering $1.2 < \eta < 2.2$, was operational for this data set. Electrons are identified by matching charged particle tracks to energy deposits in the electromagnetic calorimeter (EMC) and to rings in the ring imaging Čerenkov detector (RICH), which has a threshold of 4.7 GeV/$c$ for pions. Muons are identified by finding deeply penetrating roads in the muon identifier (MuID) and matching them to tracks in the muon tracker (MuTr).

The data were recorded during the $\sqrt{s} = 200$ GeV $pp$ run covering the end of 2001 and the beginning of 2002. After quality assurance and vertex cuts ($\pm 35$ cm for $ee$ and $\pm 38$ cm for $\mu\mu$), 67 nb$^{-1}$ were used for the $J/\psi \to \mu^+\mu^-$ analysis, and 82 nb$^{-1}$ for $J/\psi \to e^+e^-$. The minimum bias interaction trigger required at least one hit on each side of the interaction vertex in the beam-beam counter (BBC), which covers $3.1 < |\eta| < 3.9$. Minimum bias trigger rates varied from 5 to 30 kHz. Events containing $J/\psi$ decays were selected using level-1 triggers in coincidence with the minimum bias interaction trigger. The $J/\psi \to e^+e^-$ trigger required a minimum energy deposit of either 0.75 GeV in a $2 \times 2$ tile of EMC towers or 2.1 GeV in a $4 \times 4$ tile. The $J/\psi \to \mu^+\mu^-$ trigger required at least two deeply penetrating roads in separate azimuthal quadrants of the MuID [9].

$J/\psi$ yields in the central arms were obtained by reconstructing electron-positron pairs. Electron candidates were charged particle tracks that were associated with a RICH ring ($\geq 2$ hit phototubes) and an EMC hit ($\pm 4\sigma$ position association cut), and which satisfied $0.5 < E/p < 1.5$, where $E$ is the EMC cluster energy and $p$ is the reconstructed track momentum. A 5 GeV/$c$ upper limit on electron momentum prevented charged pions from firing the RICH.

$J/\psi$ yields in the muon arm were obtained by reconstructing $\mu^+\mu^-$ pairs. Muon tracks were reconstructed by finding a track seed in the MuID and matching it to clusters of hits in each of the three MuTr stations. The momentum was determined by fitting, with a correction for energy loss, the MuID and MuTr hit positions and the BBC vertex position. Each track was required to pass $5\sigma$ cuts on the $\chi^2$ from the track fit and on the radial distance of the fitted track from the measured $z$-vertex position.

Unlike-sign pairs and, for background estimation, like-sign pairs satisfying the above conditions were combined to form invariant mass spectra. Simulations show that the acceptance for like-sign and unlike-sign pairs is the same to within a few percent for invariant masses above 1 GeV/$c^2$ for electrons. In Fig. 1, unlike-sign and like-sign invariant mass spectra from the entire $pp$ data set are shown together. For electrons, the net yield inside 2.8–3.4 GeV/$c^2$ is $46 \pm 7.4$, and for muons inside 2.71–3.67 GeV/$c^2$ it is $65 \pm 9.5$. For electrons, the peak width is 110 MeV/$c^2$ and the centroid agrees well with the Particle Data Group (PDG) value [10]. For muons, the width is 160 MeV/$c^2$. The muon peak centroid is higher than the PDG value by about 3%, consistent with the uncertainty in the muon magnetic field calibration. In both cases the width of the mass window was chosen to be 6 times the standard deviation expected from simulations.

The $J/\psi$ cross sections were determined from the measured yields using

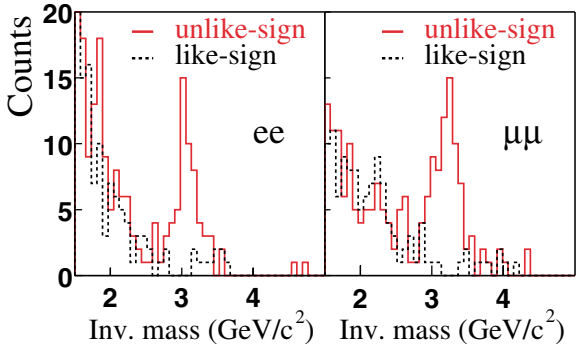


FIG. 1 (color online). The invariant mass spectra for dielectron and dimuon pairs. Unlike-sign pairs are shown as solid lines, and the sum of like-sign pairs as dashed lines.

$$B_{ll}\frac{d^2\sigma_{J/\psi}}{dydp_T} = \frac{N_{J/\psi}}{(\int \mathcal{L}dt)\Delta y \Delta p_T}\frac{1}{\epsilon_{\rm bias}\epsilon_{lvl1}}\frac{1}{A\epsilon_{\rm rec}},$$

where $N_{J/\psi}$ is the measured $J/\psi$ yield, $\int \mathcal{L}dt$ is the integrated luminosity measured by the minimum bias trigger, $B_{ll}$ is the branching fraction for the $J/\psi$ to either $e^+e^-$ or $\mu^+\mu^-$ pairs (PDG average value 5.9% [10]), $\epsilon_{\rm bias}$ is the minimum bias trigger efficiency for an event containing a $J/\psi$, $\epsilon_{lvl1}$ is the level-1 trigger efficiency for detecting a $J/\psi$, and $A\epsilon_{\rm rec}$ is the acceptance times reconstruction efficiency for a $J/\psi$.

The integrated luminosity can be written as $\int \mathcal{L}dt = N_{\rm MB}/\sigma_{\rm BBC}$, where $N_{\rm MB}$ is the number of minimum bias triggers and $\sigma_{\rm BBC}$ is the minimum bias trigger cross section. Using a van der Meer scan measurement, $\sigma_{\rm BBC}$ was determined to be $21.8 \pm 2.1$ mb [11]. We have estimated $\epsilon_{\rm bias}$ in two ways. First, the minimum bias trigger efficiency for $J/\psi$ events from a simulation study using PYTHIA [12] [with the GRV94NLO parton distribution functions (PDFs)] was 0.74, with no $p_T$ dependence. Good agreement is observed in the $dN_{ch}/d\eta$ distribution between PYTHIA simulations and measurements [13] for events involving high $p_T$ $\pi^0$ production. Second, we measured [11] our minimum bias trigger efficiency for high $p_T$ $\pi^0$ production using events recorded with a high $p_T$ EMC trigger. The efficiency of $0.75 \pm 3\%$ is constant within uncertainties over the measured range of $1.5 < p_T < 9$ GeV/$c$. We chose to use our measured trigger efficiency from high $p_T$ $\pi^0$ events when calculating the $J/\psi$ cross section, assuming that the trigger efficiency is the same for both processes.

For the electron analysis, $A\epsilon_{\rm rec}$ was determined as a function of $p_T$ using a full GEANT simulation of single $J/\psi$ events with flat distributions in $dN/dy$ ($|y| < 0.6$), $p_T$ ($p_T < 6$ GeV/$c$), and collision vertex ($|z| < 35$ cm). The GEANT simulations were tuned to match real detector responses for single electrons. The reconstruction efficiency calculations used a typical dead channel map. An average correction for run-to-run variations in detector active area was determined from single electron yields. An estimate of the systematic uncertainty in $A\epsilon_{\rm rec}$ due to $z$ vertex dependence of the acceptance, momentum resolution effects, the pair mass cut, and electron identification cuts is given in Table I, along with the uncertainty in the yield due to Drell-Yan and correlated charm decay contributions. The efficiency $\epsilon_{lvl1}$ of the level-1 $J/\psi$ triggers in the central arms was determined as a function of $p_T$ by using a software trigger-emulator to analyze simulated single $J/\psi$ events. The results are shown in Table I. The trigger emulator was tuned by analyzing simulated single electrons and comparing with the real single electron trigger efficiency.

TABLE I. Table of quantities and their systematic error estimates (in parentheses). Ranges are given for $p_T$ dependent quantities. For the $\mu^+\mu^-$ case the values of $A\epsilon_{\rm rec}$ and $\epsilon_{lvl1}$ are combined. The absolute cross section normalization uncertainty from $\epsilon_{\rm bias}$ and $\int \mathcal{L}dt$ is kept separate and is labeled (abs).

| Quantity | $e^+e^-$ | $\mu^+\mu^-$ |
|---|---|---|
| Yield | ($\pm$ 5%) | ($\pm$5%) |
| $A\epsilon_{\rm rec}$ | 0.026–0.010($\pm$13%) | 0.038–0.017($\pm$13%) |
| $\epsilon_{lvl1}$ | (2 × 2) 0.87–0.90($\pm$5%) | |
| | (4 × 4) 0.30–0.74($\pm$36%) | |
| $\epsilon_{\rm bias}$ | 0.75($\pm$3%) | 0.75($\pm$3%) |
| $\int \mathcal{L}dt$ | 82 nb$^{-1}$ ($\pm$9.6%) | 67 nb$^{-1}$ ($\pm$9.6%) |
| Total | $\pm$15%(syst) $\pm$ 10%(abs) | $\pm$14%(syst) $\pm$ 10%(abs) |

For the muon arm, $A\epsilon_{\rm rec}\,\epsilon_{lvl1}$ was determined as an average within each rapidity and $p_T$ bin, using a full GEANT simulation with $J/\psi$ events generated by PYTHIA (with GRV94LO PDFs). The PYTHIA $J/\psi$ rapidity and $p_T$ distributions are very similar to those of the real data, so that bin averaging effects should be approximately accounted for by this procedure. The simulated events were reconstructed using the same reconstruction software and cuts as for the real data, assuming nominal detector efficiencies and typical realistic dead channel and dead high-voltage maps. Each event had to pass the simulated dimuon trigger. The systematic error includes discrepancies between Monte Carlo and real detector response, run to run variations in the detector state, and uncertainties in the PYTHIA distributions. The results, integrated over the rapidity range of the muon arm, are shown in Table I, along with an estimate of the systematic error on the yield due to the background subtraction technique. In both the electron and muon cases the $J/\psi$ polarization was assumed to be zero, since existing $J/\psi$ polarization measurements are consistent with zero at low $p_T$ [14]. The effect of the unknown $J/\psi$ polarization has not been included in the systematic error.

The $p_T$ distributions for $J/\psi \to e^+e^-$ and $J/\psi \to \mu^+\mu^-$ are shown in Fig. 2, with predictions [15] from the COM. Predictions of the CSM, which greatly underpredicts the cross sections, are also shown. These

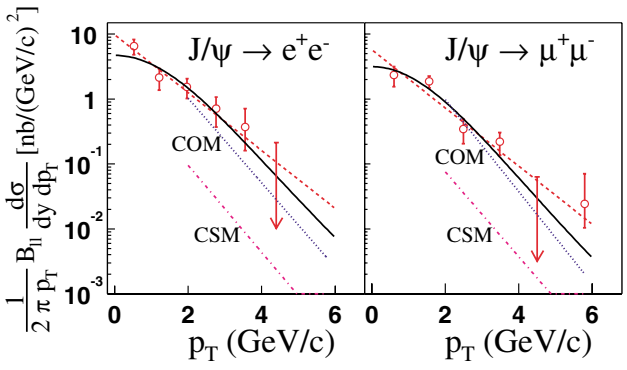


FIG. 2 (color online). The $J/\psi$ $p_T$ distributions for the dielectron and dimuon measurements, with statistical uncertainties. The solid line is a phenomenological fit of the form $(1/2\pi p_T)d\sigma/dp_T = A[1 + (p_T/B)^2]^{-6}$. The dashed line is an exponential fit. The CSM (dot-dashed) and COM (dotted) calculations are from [15].

predictions are limited to $p_T > 2$ GeV/$c$ because parton intrinsic transverse momentum ($k_T$) broadening is not accounted for properly in the calculation. The COM calculations do not include fragmentation contributions, which become important at around 5 GeV/$c$ [3]. Another calculation for the PHENIX muon arm using NRQCD is available in Ref. [16]. Calculations covering all $p_T$ and including fragmentation contributions are needed. The solid lines are a phenomenological fit of a form that has been shown to fit $J/\psi$ data well at fixed target energies [17]. The dashed line is an exponential fit. The phenomenological fits yield $\langle p_T \rangle$ values of $1.85 \pm 0.46(\text{stat}) \pm 0.16(\text{syst})$ GeV/$c$ (central arm) and $1.78 \pm 0.27(\text{stat}) \pm 0.16(\text{syst})$ GeV/$c$ (muon arm), with a combined value of $1.80 \pm 0.23(\text{stat}) \pm 0.16(\text{syst})$ GeV/$c$. The systematic uncertainties were estimated from the spread in $\langle p_T \rangle$ from a weighted mean of the binned data, the phenomenological fit, and the exponential fit. An additional 3% was assigned to the muon $\langle p_T \rangle$ due to the uncertainty in momentum scale.

The $J/\psi$ rapidity distribution obtained by combining the dielectron and dimuon measurements is shown in Fig. 3, with the muon arm data divided into two rapidity bins. The COM curves are theoretical shape predictions [9] using the same models as are discussed in connection with Fig. 4(b), except that they are normalized to our data to make the shape comparison clearer. Since gluon fusion is the dominant process in all of the models, the rapidity shape depends mostly on the gluon distribution function and is not very sensitive to the production model. Most of the available PDFs are consistent with the data, and improved statistical precision will be needed to constrain them. A PYTHIA calculation that reproduces the shape of our data best is also shown in Fig. 3. Normalizing this to the data, the total cross section was determined to be $4.0 \pm 0.6(\text{stat}) \pm 0.6(\text{syst}) \pm 0.4(\text{abs})$ $\mu$b. The quoted systematic error was estimated by setting the measured cross sections all to their upper systematic error limits or all to their lower systematic error limits and noting how the cross section changed. The variation in the total cross section extracted if we use the same procedure with different PDF choices and models was estimated to be small (3%). We note that the minimum bias trigger efficiency for a single or double diffractive event producing a $J/\psi$ will be different from the one we have assumed. However, the measured diffractive component of the $J/\psi$ cross section at $\sqrt{s} = 1.8$ TeV and $p_T > 2$ GeV/$c$ for both muons is only 1.45% [18], with little or no $p_T$ dependence, suggesting that the diffractive component should be negligible in our case.

A comparison is made in Fig. 4(a) of the present $\langle p_T \rangle$ value with values from previous experiments [1]. There are no theoretical predictions that we can compare with the $\langle p_T \rangle$ measurements. The total $J/\psi$ cross section determined in this analysis is shown in Fig. 4(b), along with cross sections determined by lower energy experiments [1] and predictions from the COM [9] using two different PDFs. The $\sqrt{s}$ dependence of the cross section is sensitive to the factorization scale $Q$, since the shape of the PDFs depends on $Q$. The values of $Q$ (3.1 GeV for GRV98NLO and 2.3 GeV for MRST2001NLO) were chosen to give good agreement with the data. The total cross section normalization was obtained using color octet matrix elements from [19], but has large theoretical uncertainties associated with the charm quark mass and the renormalization scale. The renormalization scale was taken to be equal to the quark mass $M_c$, and their values (1.48 GeV for GRV98NLO and 1.55 GeV for MRST2001NLO) were chosen to give good agreement with the data. The CEM is also able to describe the total cross section data [6]. All measurements and models include feed-down from the $\chi_c$ and the $\psi'$ to the $J/\psi$. We estimate [20] that $B$ decay feed-down contributes less than 4% to the $J/\psi$ total cross section at $\sqrt{s} = 200$ GeV.

In summary, we have presented the first $pp \to J/\psi + X$ measurements from RHIC, obtained at $\sqrt{s} = 200$ GeV. The rapidity distributions, $p_T$ distributions,

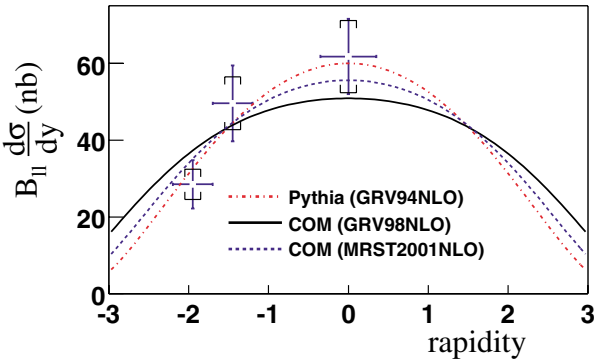


FIG. 3 (color online). The central rapidity point is from $J/\psi \to e^+e^-$, the others from $J/\psi \to \mu^+\mu^-$. The brackets represent systematic uncertainties. All curves have their overall normalization fitted to the data. The PYTHIA shape was used to determine the cross section. There is an overall 10% absolute normalization error not shown.

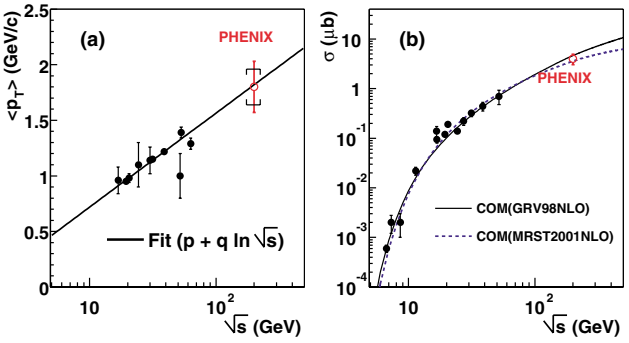


FIG. 4 (color online). (a) The present $J/\psi$ mean $p_T$ value compared with previous measurements at lower energy [1]. The linear fit parameters are $p = 0.53$, $q = 0.19$. (b) The present $J/\psi$ total cross section compared with previous measurements at other values of $\sqrt{s}$ [1]. The curves are discussed in the text.

$\langle p_T \rangle$, and total cross sections have been presented and compared with available model calculations. The transverse momentum distributions above 2 GeV/$c$ are reasonably well described by the COM. With the present statistical precision, our rapidity distribution shape is consistent with most of the available PDFs. COM calculations are able to reproduce the $\sqrt{s}$ dependence of the cross section using color octet matrix elements found in the literature, with a reasonable choice of QCD parameters.

RHIC is expected to have proton-proton runs with enhanced luminosity at $\sqrt{s} = 200$ and 500 GeV in the near future. The increased luminosity will improve the statistical precision and $p_T$ reach of the PHENIX data, and will ultimately make it possible to measure the $J/\psi$ polarization, which has been an important test for models [14].

We thank the staff of the Collider-Accelerator and Physics Departments at BNL for their vital contributions. We acknowledge support from the Department of Energy and NSF (U.S.A.), MEXT and JSPS (Japan), CNPq and FAPESP (Brazil), NSFC (China), CNRS-IN2P3 and CEA (France), BMBF, DAAD, and AvH (Germany), OTKA (Hungary), DAE and DST (India), ISF (Israel), KRF and CHEP (Korea), RMIST, RAS, and RMAE, (Russia), VR and KAW (Sweden), U.S. CRDF for the FSU, U.S.-Hungarian NSF-OTKA-MTA, and U.S.-Israel BSF.

*Deceased.
†PHENIX Spokesperson.
Email address: zajc@nevis.columbia.edu

[1] R. Vogt, Phys. Rep. **310**, 197 (1999); G. A. Schuler, hep-ph/9403387; A. Gribushin *et al.*, Phys. Rev. D **62**, 012001 (2000), and references therein.
[2] F. Abe *et al.*, Phys. Rev. Lett. **69**, 3704 (1992); F. Abe *et al.*, Phys. Rev. D **66**, 092001 (2002); S. Abachi *et al.*, Phys. Lett. B **370**, 239 (1996); B. Abbot *et al.*, Phys. Rev. Lett. **82**, 35 (1999).
[3] F. Abe *et al.*, Phys. Rev. Lett. **79**, 572 (1997).
[4] E. Braaten *et al.*, Annu. Rev. Nucl. Part. Sci. **46**, 197 (1996).
[5] G.T. Bodwin *et al.*, Phys. Rev. D **51**, 1125 (1995); **55**, 5853(E) (1997).
[6] J. F. Amundson *et al.*, Phys. Lett. B **390**, 323 (1997); (and private communication).
[7] E. Braaten *et al.*, Phys. Rev. Lett. **71**, 1673 (1993).
[8] K. Adcox *et al.*, Nucl. Instrum. Methods Phys. Res., Sect. A **499**, 469 (2003).
[9] H. D. Sato, Ph.D. thesis, Kyoto University, 2003; hep-ph/0305239.
[10] Particle Data Group, K. Hagiwara *et al.*, Phys. Rev. D **66**, 010001 (2002).
[11] S. S. Adler *et al.*, Phys. Rev. Lett. **91**, 241803 (2003).
[12] T. Sjöstrand, Comput. Phys. Commun. **135**, 238 (2001).
[13] R. Kephart *et al.*, Phys. Rev. D **14**, 2909 (1976).
[14] T. Affolder *et al.*, Phys. Rev. Lett. **85**, 2886 (2000); E. Braaten *et al.*, Phys. Rev. D **62**, 094005 (2000).
[15] G. C. Nayak, M. X. Liu, and F. Cooper, Phys. Rev. D **68**, 034003 (2003).
[16] M. Klasen *et al.*, Phys. Rev. D **68**, 034017 (2003).
[17] A. Gribushin *et al.*, Phys. Rev. D **62**, 012001 (2000), and references therein.
[18] T. Affolder *et al.*, Phys. Rev. Lett. **87**, 241802 (2001).
[19] M. Beneke and I. Z. Rothstein, Phys. Rev. D **54**, 2005 (1996).
[20] S. S. Adler *et al.*, Phys. Rev. C **69**, 014901 (2004).